JOURNAL OF MATERIALS SCIENCE **36** (2001) 1213–1217

EPR spectra of V (IV) in zirconolite-rich ceramics

L. D. BOGOMOLOVA
Institute of Nuclear Physics, Moscow State University, Moscow 119899, Russia

S. V. STEFANOVSKY, A. Y. TROOLE
SIA Radon, 7th Rostovskii per. 2/14, Moscow 119121, Russia

E. R. VANCE
ANSTO, Lucas Heights, PMB 1 Menai, NSW 2234, Australia

EPR spectra of V^{4+} in zirconolite-rich ceramics with nominal composition $Ca_{1.00}Gd_{0.01}Zr_{0.99}Ti_{1.99}V_{0.01}O_{7.00}$ were studied. It was found that these spectra contain the lines of Gd^{3+} and V^{4+} ions. Computer calculation of the spectrum of V^{4+} with hyperfine structure showed that it is a superposition of two spectra of V^{4+} ions due to V^{4+} ions substituting for Ti^{4+} ions in two non-equivalent positions of these ions in zirconolite lattice. The analysis of linewidths of hyperfine components of the V^{4+} spectrum indicates the correlated positions of Gd and V in the zirconolite lattice with the distance between them $r_{V\text{-}Gd} \sim 1$ nm. It is assumed that V^{5+} ions also substitute for Ti^{4+} ions and compensate the electric charge of Gd^{3+} ions, which replace Zr^{4+} in the same unit cell of zirconolite crystal lattice. © *2001 Kluwer Academic Publishers*

1. Introduction

According to a high level waste (HLW) partitioning concept [1], the rare earth-actinide fraction should be long-term stored being incorporated into ceramic materials with high radiation stability and chemical durability. Zirconolite with nominal formula $CaZrTi_2O_7$ is considered as one of the most promising host phase for the incorporation of actinides (An) and rare earths (REE) [2–4]. One of the major isomorphic substitution schemes in the zirconolite is $Zr^{4+} + Ti^{4+} = (REE, An)^{3+} + Me^{5+}$, where $Me^{5+} = V^{5+}, Nb^{5+}, Ta^{5+}$ [2–4]. Taking into account that some REE and An ions being of interest are paramagnetic (Gd^{3+}, Cm^{3+}) and some others can be easily reduced to lower oxidation states (Ti^{3+}, V^{4+}, Nb^{4+}) and turning paramagnetic, an electron paramagnetic resonance (EPR) technique may be applied to identify the lattice sites of waste elements and charge compensating ions in the ceramics. For example, recently some data on paramagnetic ions in the zirconolite ceramics have been reported [5, 6]. In the present work we would like to report EPR data elucidating structural positions of vanadium in the zirconolite ceramics. We investigated the samples of zirconolite with nominal composition $Ca_{1.00}Gd_{0.01}Zr_{0.99}Ti_{1.99}V_{0.01}O_{7.00}$, which contains Gd as trivalent REE and actinide surrogate, where the isomorphic substitution scheme $Zr^{4+} + Ti^{4+} = Gd^{3+} + V^{5+}$ is expected. Assuming that vanadium is present in ceramics mainly as V^{5+} ions we recorded for comparison the EPR spectrum of $Ca_{1.00}Gd_{0.01}Zr_{0.99}Ti_{1.99}Ta_{0.01}O_{7.00}$ containing Ta^{5+} ($Zr^{4+} + Ti^{4+} = Gd^{3+} + Ta^{5+}$) as well as the spectrum of zirconolite with formula $Ca_{0.995}Gd_{0.01}Zr_{0.995}Ti_{2.00}O_{7.00}$ not containing pentavalent elements.

2. Experimental

The samples examined were prepared by ceramic and melting routes.

The ceramic route included the preparation of precursor from Ti, Zr, V, Ta and Al alkoxides, and Ca and Gd nitrates, calcination at 750 °C for 1 h in air, wet ball-milling for 16 h, pelletization and sintering at 1400 °C for 16 h.

The melting route was as follows. Oxide/nitrate mixtures were milled and blended in an agate mortar, placed in a platinum crucible, heated in a resistive furnace to 1550 °C for 4 h, kept at this temperature for 30 min, cooled to 1000 °C for 3 h, and followed by cooling down to room temperature overnight.

The samples obtained were examined with X-ray diffraction (XRD) using a DRON-4 diffractometer (Cu Kα - radiation) and scanning electron microscopy equipped with energy dispersive system (SEM/ESD) using a JSM-5300 + Link ISIS Analytical System.

EPR spectra were recorded at room temperature with a Bruker ESP-300 spectrometer operating at X-band frequency.

3. Results

As follows from XRD and SEM/EDS data, zirconolite-2M (monoclinic) is the major phase in the samples prepared by both sintering and melting with the composition corresponding to the starting stoichiometry. The melted V-doped sample also contains rare grains of zirconia.

Fig. 1 shows the EPR spectra of $Ca_{0.995}Gd_{0.01}Zr_{0.995}Ti_2O_7$ (a), Ta-doped (b,c) and V-doped (d,e) samples. As can be seen the spectra presented on Fig. 1a, b,

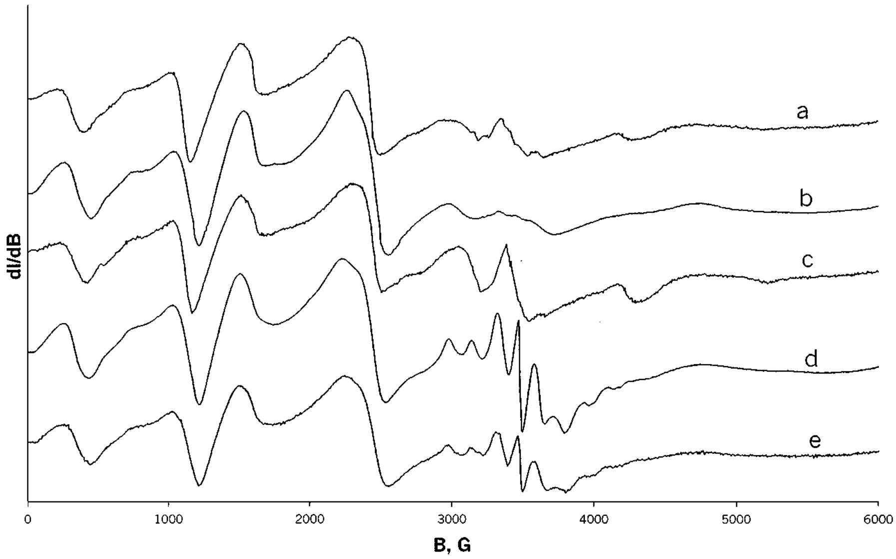

Figure 1 EPR spectra of the zirconolite ceramic samples $Ca_{0.995}Gd_{0.01}Zr_{0.995}Ti_2O_7$ (a), $CaGd_{0.01}Zr_{0.99}Ti_{1.99}Ta_{0.01}O_7$ (b,c), and $CaGd_{0.01}Zr_{0.99}$-$Ti_{1.99}Ta_{0.01}O_7$ (d,e) produced by melting (a,c,e) and sintering (b,d).

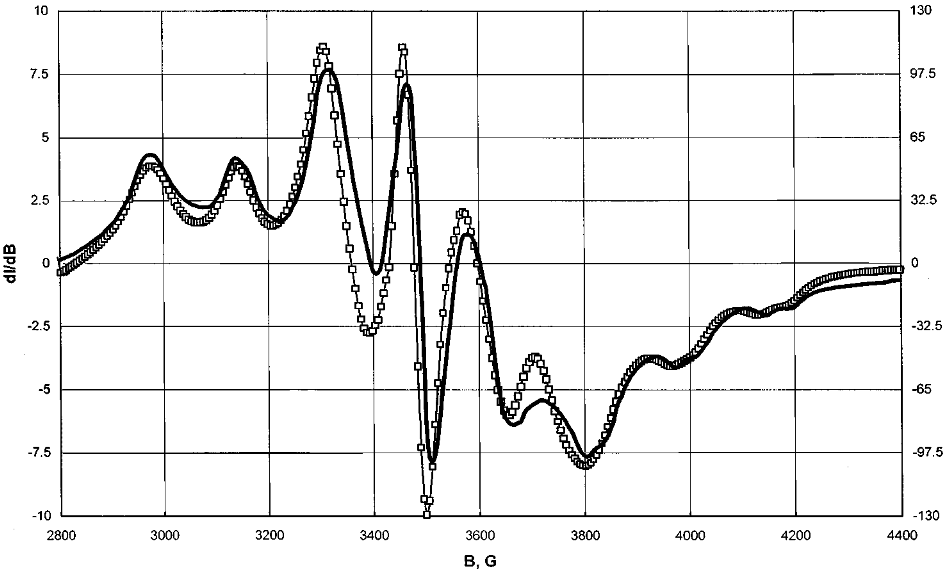

Figure 2 Experimental (solid curve) and calculated (squares) spectra of V^{4+} in zirconolite ceramics.

and c are similar, i.e. these spectra, including the spectra of Ta-doped samples, are due to Gd^{3+} ions. No signal due to Ta^{4+} was found.

In the central part of the spectra of the V-doped ceramics produced by both sintering and melting the spectrum due to V^{4+} is superimposed on the Gd^{3+} spectrum (Fig. 1d and e). Even though the vanadium and gadolinium concentrations are equal (0.01 formula unit for each) the Gd^{3+} spectrum is much more intense than the V^{4+} spectrum.

Fig. 2 (solid curve) shows the central part of the EPR spectrum of the V-doped sample. The contribution to this spectrum due to V^{4+} ions exhibit several components of hyperfine structure (HFS) due to the interaction between the unpaired electron and magnetic moment of the ^{51}V nuclei ($I = 7/2$). As can be seen, some HFS lines in the high-field part of the spectrum are split into two components, indicating the presence of two non-equivalent sites of V^{4+} ions in this sample.

4. Computer simulation of the spectrum of V^{4+}

Double computer integration of the whole spectra shown in Fig. 1b and c and of their parts over the range between 2800 and 4400 G allows us to estimate the ratio of concentration of V^{4+} to V_{total} as ~5%. The major fraction of vanadium is presumably present as V^{5+} ions.

Computer simulation of the spectrum was performed. The calculated spectrum presented in Fig. 2 (squares) was obtained as a superposition of three spectra (Fig. 3). Two of them (1 and 2) were calculated for V^{4+} ions whereas the spectrum 3-4 is the region of the experimental spectrum observed for the Ta-doped sample (Fig. 1b). The spectrum 3-4 (Fig. 3) which was used for simulation of the EPR spectrum of the studied sample includes two lines due to the spectrum of Gd^{3+} ions.

Both spectra of V^{4+} ions were calculated assuming that they are described by a spin Hamiltonian of

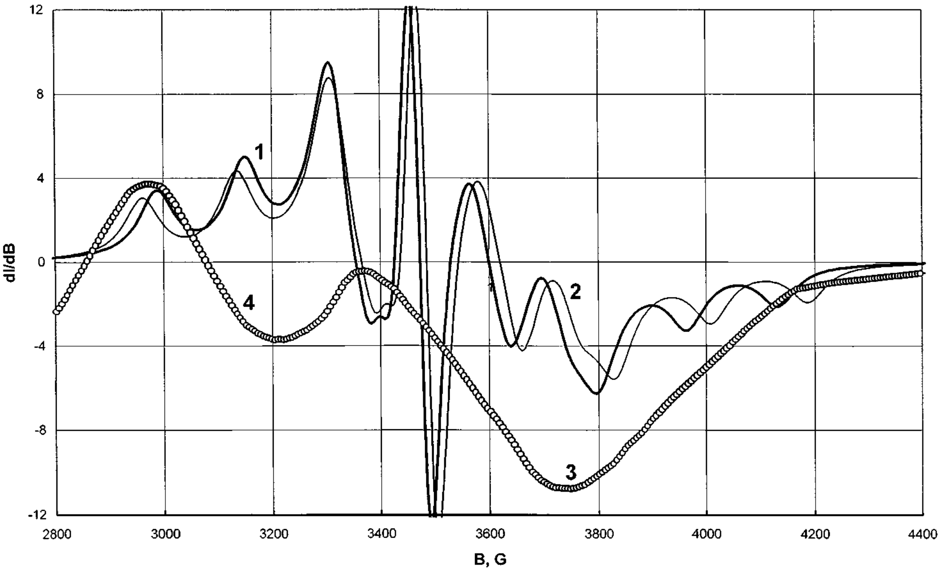

Figure 3 EPR spectra used for computer simulation of the spectrum shown in Fig. 2. 1,2 – EPR spectra of V^{4+} ions, 3-4 – residual lines due to Gd^{3+} ions.

orthorhombic symmetry with electron spin $S = 1/2$ and nuclear spin $I = 7/2$:

$$H = \beta(g_z H_z S_z + g_x H_x S_x + g_y H_y S_y) + A_z I_z S_z + A_x I_x S_x + A_y I_y S_y \quad (1)$$

The synthetic spectra of V^{4+} were computed in the form [7]:

$$S'(H) = \sum_{m-7/2}^{+7/2} \iint W(\theta, \varphi) F'_m(H, \theta, \varphi) \sin\theta \, d\theta \, d\varphi \quad (2)$$

where $W(\theta, \varphi)$ is the orientation-dependent transition probability [8]. $S'(H)$ is the first derivative of EPR absorption spectrum. To second order in perturbation theory, the resonance condition for g and hyperfine tensors [8, 9] is:

$$\begin{aligned} H(\theta, \varphi, m_I) &= h\nu/g\beta - K m_I/g\beta \\ &\quad - \left\{A_\perp^2 (A_z^2 + K^2) / \left[4g\beta^2(g_0 H_0 - Km/\beta)K^2\right] \right. \\ &\quad \times \left[I(I+1) - m^2\right]\big\} - \left\{(A_z^2 - A_\perp^2) / \left[2g\beta^2(g_0 H_0 \right.\right. \\ &\quad \left.\left. - Km/\beta)K^2\right]\right\} (g_z g_\perp / g^2)^2 \sin^2\theta \cos^2\theta \cdot m^2 \quad (3) \end{aligned}$$

where

$$\begin{aligned} g^2 &= g_z^2 \cdot \cos^2\theta + g_\perp^2 \sin^2\theta; \\ g_\perp^2 &= g_x^2 \cos^2\varphi + g_y^2 \sin^2\varphi \end{aligned} \quad (4)$$

and

$$\begin{aligned} K^2 g^2 &= A_z^2 g_z^2 \cdot \cos^2\theta + A_\perp^2 g_\perp^2 \sin^2\theta; \\ A_\perp^2 g_\perp^2 &= A_x^2 g_x^2 \cdot \cos^2\varphi + A_y^2 g_y^2 \cdot \sin^2\varphi \end{aligned} \quad (5)$$

Here m_I is nuclear magnetic quantum number, which has values from I to $-I$ where $I = 7/2$ is the nuclear spin of ^{51}V.

Functions $F'_m(H, \theta, \varphi)$ are first derivatives of individual absorption lines. We have employed the Gaussian shape of individual lines.

Summation was made for θ angle to $\pi/2$ and for φ angle to π with step 1°.

The best-fit parameters of spin-Hamiltonian are $g_z = 1.942 \pm 0.002$; $g_x = 1.957 \pm 0.002$; $g_y = 1.963 \pm 0.002$; $A_z = (148 \pm 2) \cdot 10^{-4}$ cm^{-1}, $A_x = (52 \pm 3) \cdot 10^{-4}$ cm^{-1} and $A_y = (44 \pm 3) \cdot 10^{-4}$ cm^{-1} for the spectrum **1** and $g_z = 1.934 \pm 0.002$; $g_x = 1.948 \pm 0.002$; $g_y = 1.952 \pm 0.002$; $A_z = (158 \pm 2) \cdot 10^{-4}$ cm^{-1}, $A_x = (53 \pm 3) \cdot 10^{-4}$ cm^{-1} and $A_y = (43 \pm 3) \cdot 10^{-4}$ cm^{-1} for the spectrum **2**. The widths of individual lines were $\triangle H_z = \triangle H_x = \triangle H_y = 7$ mT. Both spectra have the equal intensities.

5. Discussion

The fact that the EPR spectra of V^{4+} in the zirconolite ceramic samples prepared by two different routes are similar and the ratio of intensities of both components (Fig. 3) contributing to the whole spectra of V^{4+} (Fig. 2) is 1 : 1 indicates two well-defined non-equivalent positions of V^{4+} ions. This is possible if V^{4+} ions substitute for ions occupying two different sites in crystal lattice. As follows from Ref. [10] only titanium occupies two distinct sites in zirconolite. Therefore, we assume that V^{4+} ions replace Ti^{4+} ions in the zirconolite lattice. Numerous EPR and NMR investigations (see, for example [11]) have shown that V^{4+} and V^{5+} ions in different materials at low concentration of V^{4+} with respect to one of V^{5+} ions have generally similar oxygen environments. Therefore, we assume that in zirconolite V^{5+} ions also substitute for Ti^{4+}.

In confirmation of our assumption we can compare the spin Hamilton parameters of V^{4+} ions in zirconolite and the other compounds [12–17].

The most typical parameters of spin Hamiltonian obtained for V^{4+} in some oxide crystals are given in Table I. As follows from reference data a local environment of V^{4+} ions in such crystals is formed by

TABLE I Some typical parameters of spin Hamoltonian of V^{4+} in oxide compounds

Nos	Crystal	Coordination	Symmetry	Ground state	g_z	g_y	g_x	A_z	A_y	A_x	Ref.
1.	Tutton salts and alums	Octahedral	C_{4v}	xy	1.931–1.941	1.975–1.999	1.975–1.996	176–184	62–74	66–75	12
2.	$MgRb_2(SO_4)_2$ $6H_2O$	Octahedral	C_{4v}	xy	1.934	1.984	1,984	182	71	71	13
3.	Rb_2SO_4	Octahedral	C_{4v}	xy	1.961	1.974	1.974	146	67	67	12
4.	V_2O_5	Octahedral	C_{4v}	xy	1.923	1.986	1.986	168	62	62	14
5.	TiO_2 (rutile)	Octahedral	D_{2h}	x^2-y^2	1.915	1.913	1.956	31	43	142	15
6.	$ZrSiO_4$	Tetrahedral	D_{2d}	xy	1.893	1.969	1.969	81.6	28.9	28.9	16
7.	Ba0-V_2O_5 (glass)	Octahedral	C_{4v}	xy	1.930	1.972	1.972	159	52	52	17
8.	Zirconolite ceramics	Octahedral **1**	C_{4v}	xy	1.934	1.948	1.952	158	53	43	Present work
		Octahedral **2**	C_{4v}	xy	1.942	1.957	1.963	148	52	44	Present work

Note: HFS constants are expressed in 10^{-4} cm^{-1}.

compressed or elongated octahedron as well as by tetrahedron. In the case of tetrahedral coordination (for example, in zircon or zircon-structured crystals) EPR spectra of V^{4+} are observable at temperature of liquid helium or nitrogen because of short spin-lattice relaxation. Since the EPR spectra of V^{4+} ions in the zirconolite ceramics are observed at room temperature we can eliminate the possibility of tetrahedral coordination of V^{4+} ions in this material.

Information concerning the local environment of V^{4+} can be also extracted from EPR spectral parameters. For example, for crystals with rutile structure, where V^{4+} is in an elongated octahedron, the ground state of V^{4+} is a mixture of $|x^2 - y^2\rangle$ and $|z^2\rangle$ functions leading to relationship $g_\parallel > g_\perp$ with $A_\parallel > A_\perp$ whereas for V^{4+} in compressed octahedron of C_{4v} symmetry with the ground $|xy\rangle$ state $g_\parallel < g_\perp$ at $A_\parallel > A_\perp$. The most typical compressed octahedron occurs in the vanadyl complex VO^{2+} with one short $V = O$ bond (distance $R \sim 0.16$ nm), which is generally coordinated with other groups. For example, the complex $[VO(H_2O)_5]^{2+}$ ion having six-fold coordination occurs frequently and has tetragonal symmetry C_{4v} in which coplanar bonds are formed between vanadium ion and each of four planar ligands ($r_{\text{v-o}} = 0.23$ nm). The vanadyl oxygen is attached axially above the equatorial plane ($r_{\text{v-o}} = 0.167$ nm) and the most distant sixth ligand lies opposite vanadyl oxygen ($r_{\text{v-o}} = 0.24$ nm). In this case the EPR spectra exhibit axially symmetric g and HFS tensors.

Distortions from pure C_{4v} symmetry are expected to cause the deviation from axial symmetry of *A*- and *g*-tensors but the conservation of VO^{2+} as a distinct group requires that the difference between spin Hamiltonian parameters parallel and perpendicular to V=O bond remains relatively large in comparison to the difference between two perpendicular values [12].

The relationship between the parameters of spin Hamiltonian given in Table I for the zirconolite ceramics indicates that V^{4+} ions are positioned in compressed octahedra with point symmetry close to C_{4v} for both structural positions responsible for the two spectra shown in Fig. 3.

As follows from Table I, the spin Hamiltonian parameters of V^{4+} in hydrated crystals (Tutton salts, alums, etc [12, 13]) are in a rather narrow range indicating the formation of aqua complexes of vanadyl since the distances between divalent cations (M^{2+}) replaced by VO^{2+} ions and H_2O molecules are sufficient for the adaptation of such complexes. For example, in Tutton salts these distances vary from 0.1961 to 0.2298 nm [13]. The increase in V-O distances in the equatorial plane of such complexes is generally accompanied by an increase in A_z and a decrease in g_z. For example, the increase of bond length M^{2+}-O from 0.2019 to 0.2138 nm leads to the increase in A_z (in 10^{-4} cm^{-1}) from 177 to 183 [18].

When VO^{2+} is coordinated only by oxygen atoms, the range of its parameters becomes larger. However, for the majority of them the correlation between changes in A_z and g_z remains. As follows from Table I, g_z increases and A_z decreases for non-hydrated $RbSO_4$ crystal in comparison with similar hydrated compound. Such changes in the parameters are due to a decrease in a distance between vanadium and oxygen ligands in non-hydrated compounds. The calculations [19] showed that in oxide glasses g_z decreases from 1.946 to 1.928 and A_z increases from 167 to178 (in 10^{-4} cm^{-1}) when the V-O distance increases from 0.212 to 0.229 nm.

At the same time there are oxide compounds for which *g*-values are similar to those of vanadyl aqua complexes ($g_z \sim 1.93$–1.94) whereas HFS constants are essentially smaller ($\sim(150$–$160) \cdot 10^{-4}$ cm^{-1}). This behavior can be due to the considerable distortions of oxygen octahedra and changes in interatomic distances V-O for these compounds in comparison with hydrated crystals. For example, in orthorhombic V_2O_5 distances between vanadium and oxygens are $r_1 = 0.158; r_2 = 0.178; r_3 = r_4 = 0.188; r_5 = 0.202$ and $r_6 = 0.278$ (in nm) [14]. As follows from Table I, $A_z = 168 \cdot 10^{-4}$ cm^{-1} at $g_z = 1.923$ is observed for this crystal whereas for vanadyl-type complexes $A_z \sim 185 \cdot 10^{-4}$ cm^{-1} corresponds to such a g_z - value. Neutron diffraction investigation of vanadate glasses [20], which can be attributed to the same kind of compounds (see Table I), showed that the value

$r_{\text{V-o}} \sim 0.18$–0.19 nm. Therefore, we assume that the g_z value ranging between 1.925 and 1.94 together with $A_z = (145\text{–}165) \cdot 10^{-4}\ \text{cm}^{-1}$ belongs to V^{4+} ions in the distorted oxygen octahedron with interionic distances in equatorial plane $r_{\text{V-o}} \leq 0.2$ nm.

As follows from Table I, spectral parameters of V^{4+} in the zirconolite ceramics are within this range. It suggests that V^{4+} can replace titanium in the lattice of zirconolite since the mean interatomic Ti-O distances vary from 0.193 to 0.2006 nm [10].

The most remarkable feature of the spectra of V^{4+} in the zirconolite ceramics is great widths of individual lines used for their simulation ($\triangle H = 7$ mT), which are non-typical of non-magnetic crystals with low concentration of V^{4+}. The broadening of lines can be due to spin-spin interactions between V^{4+} and Gd^{3+} ions.

According to Ref. [21] the contribution to second moment of the line $\langle \triangle H^2 \rangle$ of V^{4+} ions interacting with unlike ions (Gd^{3+}) can be written as:

$$\langle \triangle H^2 \rangle = (1/3) g^2 \beta^2 S(S+1) \cdot 8.5\, d^{-6}, \qquad (6)$$

where g and S are g-factor and spin of Gd^{3+}, respectively; d is the dimension of the simple cubic lattice formed by Gd^{3+} ions around V^{4+}ion. Taking into account the dimensions of the unit cell of zirconolite ($\sim$1 nm [10]) and concentration of Gd in our samples we can estimate d-value as $d \sim 2.35$ nm. Then, $\triangle H = 0.95$ mT $\ll 7$ mT used in the calculated spectra. This means that positions of V^{4+} and Gd^{3+} in the zirconolite lattice are correlated.

Assuming that the energy of the dipole-dipole interaction between V^{4+} and Gd^{3+} is

$$E = \mu_V \mu_{Gd} \cdot r^{-3}, \qquad (7)$$

where μ_V and μ_{Gd} are magnetic moments of V^{4+} and Gd^{3+} ions, respectively, we can evaluate the distance $r_{\text{V-Gd}}$ between them leading to $\triangle H = 7$ mT using Equation 8:

$$\begin{aligned} r &= \{[g\beta \sqrt{S_1(S_1+1)S_2(S_2+1)}]/\triangle H\}^{-3} \\ &= 0.97\ (\text{nm}), \qquad (8) \end{aligned}$$

i.e. V^{4+} and Gd^{3+} enter the same unit cell of zirconolite.

Since V^{4+} ions are usually present in ceramics and glasses due to reduction of V^{5+} ions at elevated temperatures, these ions occupy the same sites. Therefore, having correlation between Gd and V ions concentrations in the zirconolite unit cell and evidence for incorporation of V ions in the Ti sites, we have to suggest coupled incorporation of Gd ions in the Zr sites for charge compensation. The results obtained are applicable for both sintered and melted samples. Therefore, the isomorphic substitution scheme $Zr^{4+} + Ti^{4+} = (REE, An)^{3+} + Me^{5+}$ is apparently realized in both the samples, in agreement with Ref. [2].

The mechanism of charge compensation at charge imbalance due to occurrence of fraction of V as V^{4+} is under discussion. This may be either $2V^{5+} = 2V^{4+} +$ oxygen vacancy or incorporation of minor Gd ($\sim$5% of total) in the Ca or Ti site.

6. Conclusion

It is shown that in zirconolite-rich ceramics doped with Gd and V with nominal composition $Ca_{1.00}Gd_{0.01}Zr_{0.99}Ti_{1.99}V_{0.01}O_{7.00}$ EPR spectra consist of lines due to Gd^{3+} and V^{4+}. From EPR data, the concentration ratio of V^{4+} to V_{total} is of order 5%. It has been found that V^{4+} substitutes for Ti^{4+} ions in two structurally non-equivalent sites. The positions of V and Gd in the zirconolite lattice are correlated. The distance between these ions estimated from width of hyperfine lines of EPR spectrum of V^{4+} is $\sim$1 nm indicating occurrence of these ions in the same unit cell. V^{4+} ions, serving as spin probe, occupy the same sites in the zirconolite structure as V^{5+} ions.

References

1. V. N. ROMANOVSKI, I. V. SMIRNOV and A. YU. SHADRIN, in *Spectrum '98, Proc. Int. Conf.* (ANS, La Grange Park, 1998), Vol. 1, p. 576.
2. E. R. VANCE, B. D. BEGG, R. A. DAY and C. J. BALL, *Mat. Res. Soc. Symp. Proc.* **353** (1995) 767.
3. E. R. VANCE, A. JOSTSONS, R. A. DAY, C. J. BALL, B. D. BEGG and P. J. ANGELL, *ibid.* **412** (1996) 41.
4. N. P. LAVEROV, B. I. OMELIANENKO, S. V. YUDINTSEV and B. S. NIKONOV, *Geol. Ore Deposits* **38** (1996) 387.
5. O. A. KNYAZEV and S. V. STEFANOVSKY, in *Proceedings of the 6th International Conference on Radioactive Waste Management and Environment Remediation ICEM'97* (ASME, New York, 1997) p. 333.
6. A. Y. TROOLE and S. V. STEFANOVSKY, *Mat. Res. Soc. Symp. Proc.* **556** (1999) 35.
7. L. D. BOGOMOLOVA, A. N. KHABAROVA, E. V. KLIMASHINA, N. A. KRASIL'NIKOVA and V. A. JACHKIN, *J. Non-Cryst. Solids* **103** (1988) 319.
8. A. ABRAGAM and B. BLEANEY, "Electron Paramagnetic Resonance of Transition Ions" (Clarendon Press, Oxford, 1970).
9. I. V. OVCHINNIKOV and V. N. KONSTANTINOV, *J. Magn. Res.* **32** (1978) 179.
10. B. M. GATEHOUSE, I. E. GREY, R. J. HILL and H. J. ROSSELL, *Acta Cryst. B* **37** (1981) 306.
11. C. N. GREEVES, *J. Non-Cryst. Solids* **11** (1973) 427.
12. R. P. KOHIN, *Magnetic Resonance Rev.* **5** (1979) 75.
13. K. JAIN and P. VENKATESWARLU, *J. Chem. Phys.* **73** (1980) 30.
14. A. KAHN, J. LIVAGE and R. COLLONGUES, *Phys. Stat. Solidi (a)* **26** (1974) 175.
15. D. P. MADASCI, R. H. BARTRAM and O. R. GILLIAM, *Phys. Rev. B* **7** (1973) 1817.
16. D. BALL and B. M. WANKLYN, *Phys. Stat. Sol. (a)* **36** (1976) 307.
17. L. D. BOGOMOLOVA, V. A. JACHKIN, M. P. GLASSOVA and S. N. SPASIBKINA, *J. De Phys.* **42** (1981) C4-993.
18. M. NARAYANA, *J. Chem. Phys.* **72** (1980) 4255.
19. H. HECHT and T. S. JONSTON, *ibid.* **46** (1967) 23.
20. A. C. WRIGHT, C. A. YARKER and P. A. V. JOHNSON, *J. Non-Cryst. Solids* **76** (1985) 333.
21. S. A. AL'TSHULER and B. M. KOZYREV "Electron paramagnetic resonance" (Moscow, 1961).

Received 6 March
and accepted 18 August 2000